

Original Article

Overexpression of miR-30a in lung adenocarcinoma A549 cell line inhibits migration and invasion via targeting *EYA2*

Yuncang Yuan^{1,†}, Shangyong Zheng^{1,†}, Qian Li¹, Xudong Xiang², Tangxin Gao¹, Pengzhan Ran¹, Lijuan Sun¹, Qionglin Huang¹, Fei Xie¹, Jing Du¹, and Chunjie Xiao^{1,*}

¹School of Medicine, Yunnan University, Kunming 650091, China, and ²Department of Thoracic Surgery, Third Affiliated Hospital of Kunming Medical University, Kunming 650118, China

[†]These authors contributed equally to this work.

*Correspondence address. Tel: +86-13888455098; Fax: +86-871-65034636; E-mail: chjxiao@ynu.edu.cn

Received 23 June 2015; Accepted 23 November 2015

Abstract

MicroRNAs (miRNAs) are a class of small non-coding RNAs and closely related to the pathogenesis of cancers. Increasing evidence indicates that miR-30a plays a profound role during the development of cancers. However, the functions of miR-30a in non-small-cell lung cancer (NSCLC) are still ambiguous. Here we found that miR-30a was decreased in lung adenocarcinoma A549 cells and in tissue samples from 14 patients by qRT-PCR, and also found that overexpression of miR-30a in A549 cells inhibited migration and invasion but not cell proliferation and cell cycle progression by wound-healing assay, matrigel invasion assay, MTS-based cell proliferation assay, and flow cytometry-based cell cycle analysis, respectively. We further explored the potential mechanism of miR-30a-mediated gene regulation in lung adenocarcinoma cell lines. *EYA2* is a predicted target of miR-30a, and it has been found that *EYA2* expression is inhibited by miR-30a in breast cancer cells. We demonstrated that *EYA2* is a direct target of miR-30a by using the dual-luciferase reporter assay in A549 cells and showed that *EYA2* protein levels are inversely correlated with miR-30a expression in A549 and BEAS-2B cells. In addition, we also confirmed the rescue effects of *EYA2* overexpression in A549 cells by cotransfection with *EYA2* expression vector and miR-30a mimics. Taken together, our results demonstrate that overexpression of miR-30a in lung adenocarcinoma A549 cells can inhibit cell migration and invasion, which is partially attributed to the decrease of *EYA2* expression. Our findings suggest that miR-30a may be used as a new potential target for the treatment of lung adenocarcinoma in the future.

Key words: lung adenocarcinoma, miR-30a, migration, invasion, *EYA2*

Introduction

Lung cancer is the main cause of cancer mortality in China, with an incidence of about 53.57 per 100,000 and a very high mortality in the registered areas in 2012 [1]. Non-small-cell lung cancer (NSCLC), including adenocarcinoma, squamous carcinoma, and large cell carcinoma, is the main histological type of the lung cancer

and accounts for nearly 80% of the lung cancer. Despite new drugs and therapeutic regimens, the overall five-year survival rate of NSCLC patients is still low at ~15% at present. Effective therapeutic strategies are urgently needed for the NSCLC treatment.

miRNAs are a class of conserved, 19–24 nucleotides long, non-coding small RNAs which act by fine-tuning gene expression through

a post-transcriptional mechanism. It is clear now that miRNAs perform their biological functions by guiding the RNA-induced silencing complex (RISC) toward 3' UTR of target mRNAs [2]. miR-30a locates in human chromosome 6q13 and increasing evidence indicates that miR-30a can act as a tumor suppressor to inhibit the growth of various tumors including colorectal carcinoma [3–5], breast cancer [6], anaplastic thyroid cancer [7], Ewing's tumor [8], clear cell renal cell carcinoma [9], gastric cancer [10], and nasopharyngeal carcinoma [10,11]. In addition, miR-30a also shows the feature of an oncogene. One study about glioma showed that miR-30a can promote tumor cell growth [12]. In a recent study, researchers also demonstrated the function of miR-30a as an oncogene in ovarian granulosa cell tumor [13]. Together, these data indicate that the regulatory roles of miR-30a vary in different cancers. Currently, limited information concerning the biological functions of miR-30a in NSCLC has been reported. High-throughput screening results indicated that miR-30a expression was decreased in the NSCLC [14], but this may not be associated with the cell cycle, proliferation, xenograft formation, and chemosensitivity of A549 cells [15]. Considering the complexity of miRNAs' regulation in cancers and the potential value of miRNAs in cancer treatment, further research is needed to address the functional consequence of abnormal miR-30a expression in the pathogenesis of NSCLC.

EYA2 is a member of the *EYA* family proteins. As a novel class of protein tyrosine phosphatases (PTPs) [16], *EYA2* has been reported to promote the proliferation, transformation, migration, and invasion of breast cancer [6,17]. The allosteric inhibitors of the *EYA2* phosphatase had also been reported to inhibit *EYA2*-mediated cell migration in breast cancer [18]. Moreover, the abnormal expression of *EYA2* was also found in other cancers such as cervical cancer [19], pancreatic adenocarcinoma [20], colorectal neoplasia [21], epithelial ovarian cancer [22], and particularly NSCLC [23]. A recent study demonstrated that *EYA2* is a direct target of miR-30a in breast cancer [6]. Given that the mechanisms of miR-30a in NSCLC are still ambiguous, it is valuable to elucidate the relationship between miR-30a and *EYA2* in NSCLC.

In this study, the biological effects of miR-30a were studied in lung adenocarcinoma A549 cells. In addition, to provide more evidence for elucidating the mechanism of miR-30a in the pathogenesis of lung adenocarcinoma, *EYA2* as a potential target of miR-30a was also explored in lung adenocarcinoma A549 cells. Our results indicated that overexpression of miR-30a in lung adenocarcinoma A549 cell line inhibited migration and invasion, which could partially be attributed to the decrease of *EYA2* expression.

Materials and Methods

Ethics statement

The study was approved by the Medical Ethics Committee of the School of Medicine Yunnan University (Kunming, China). Human samples were used in accordance with the requirement of Medical Ethics Committee of the School of Medicine Yunnan University. All patients provided written informed consent.

Tissues

Paired lung adenocarcinoma and adjacent normal tissues were obtained with diagnostic information from 14 patients who were diagnosed as lung adenocarcinoma from 2012 to 2013 at the No.1 School of Clinical Medicine, Kunming Medical University. All samples were formalin-fixed routinely and paraffin embedded (FFPE).

Cell culture and transfection

A549 lung carcinoma cells from the Tumor Hospital of Yunnan Province (Kunming, China) and BEAS-2B normal lung/bronchus epithelial cells from the Conservation Genetics CAS Kunming Cell Bank (Kunming, China) were cultured in Dulbecco's modified Eagle medium (DMEM; Thermo Fisher Scientific, Rockford, USA) or Roswell Park Memorial Institute 1640 medium (Thermo Fisher Scientific) with 10% fetal bovine serum (FBS; Life Technologies, Grand Island, USA), 100 µg/ml streptomycin and 100 U/ml penicillin (Thermo Fisher Scientific). For functional analysis, siRNAs negative control (siRNAs NC), *EYA2* siRNAs, inhibitors negative control (inhibitors NC), mimics negative control (mimics NC), miR-30a mimics, and miR-30a inhibitors (GenePharma, Shanghai, China) were transfected, respectively, into cells using HiPerFect Transfection Reagent (QIAGEN, Hilden, Germany). Plasmids and miR-30a mimics/mimics NC were cotransfected into cells using Attractene Transfection Reagent (QIAGEN). The transfection was done according to the manufacturer's protocols.

Total RNA isolation and miRNA qRT-PCR analysis

Total RNA was extracted from FFPE tissues using the miRNeasy FFPE Kit (QIAGEN) and from cell lines using Trizol reagent (TaKaRa, Dalian, China) according to the manufacturer's instructions. The stem-loop primer quantitative real-time polymerase chain reaction (qRT-PCR) method described by Chen *et al.* [24] was used to examine the expression level of endogenous miR-30a in lung tumor cells and tissues. U6 snRNA was chosen as an internal control. The primers used for PCR were as follows: miR-30a stem-loop primer, 5'-CAC AGCGGCTGTCGTTGACTGCGTGCTGCCGCTGTGCTTCCA-3';

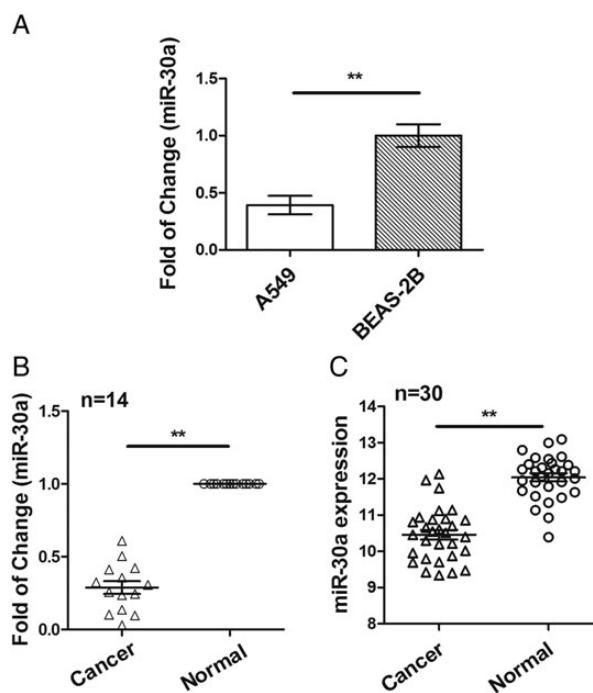


Figure 1. miR-30a is down-regulated in the lung adenocarcinoma cell line of A549 and adenocarcinoma tissues (A) The expression level of miR-30a in A549 and BEAS-2B cells was evaluated by qRT-PCR. U6 snRNA was used as an internal control. (B) The expression level of miR-30a in 14 pairs of adenocarcinoma tissues and their matched normal lung tissues were evaluated by qRT-PCR. U6 snRNA was used as an internal control. (C) The datasets GSE63805 searched from GEO were used for miR-30a expression analysis. ** $P < 0.01$.

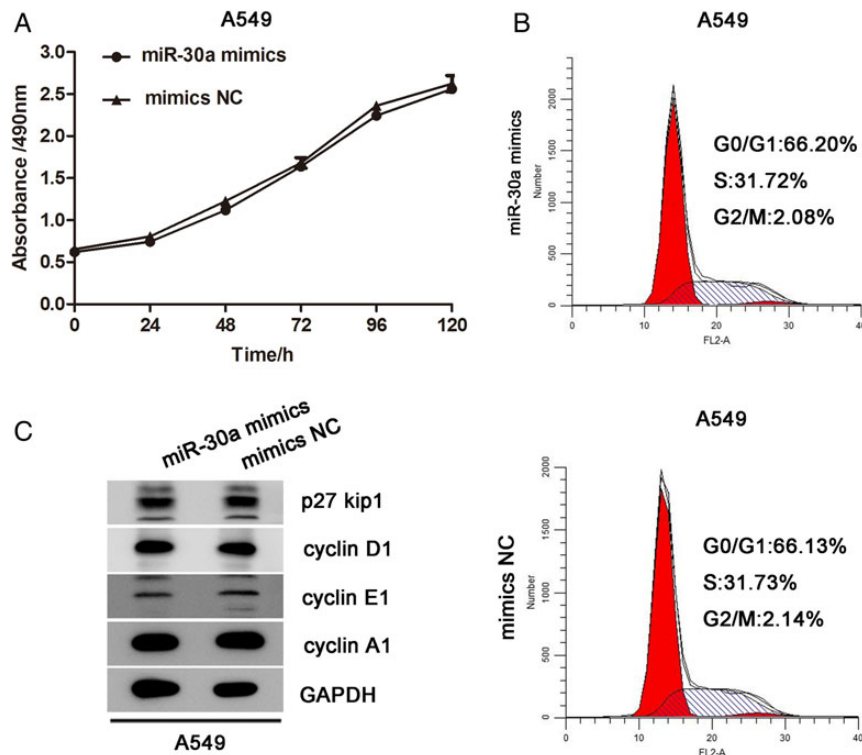


Figure 2. Overexpression of miR-30a in A549 cells has no effect on the cell proliferation and cell cycle distribution. (A) For cell proliferation analysis, A549 cells were transfected with 20 nM mimics NC or miR-30a mimics, respectively. Twenty-four hours after transfection, cells were collected and seeded into a 96-well plate (1000 cells per well), and cultured for 120 h. The growth of the cells was analyzed by MTS assay, and all values were shown as the mean \pm SE of triplicate measurements. (B) A549 cells were transfected with 20 nM mimics NC or miR-30a mimics, respectively, as indicated. Forty-eight hours later, 10^6 cells were collected for cell cycle analysis by PI staining and flow cytometer assay. (C) Western blot analysis of p27 kip1, cyclin D1, cyclin E1, and cyclin A1 in A549 cells after transfection with 20 nM mimics NC or miR-30a mimics. GAPDH was used as a loading control. All experiments were repeated at least three times with similar trends.

miR-30a forward primer, 5'-AGACCCGTGTAAACATCCTCG-3'; miR-30a reverse primer, 5'-GGCTGTCGTTGACTGCGTG-3'; U6 forward primer, 5'-CTCGCTTCGGCAGCACA-3'; and U6 reverse primer, 5'-AAGCCTTCACGAATTTGCGT-3'. cDNA was synthesized by using the RT reagent kit (TaKRa), and PCR was performed by using SYBR Green real-time kit (TaKRa) in the ABI 7300 real-time PCR system (Life Technologies) with the following reaction conditions: initial denaturation at 95°C for 2 min, followed by 40 cycles at 95°C for 30 s, 60°C for 40 s, and then the dissociation curve was drawn.

Cell cycle analysis

The A549 cells grown to 80%–90% confluence were detached by trypsinization at 48 h after transfection with 20 nM miR-30a mimics or mimics NC, fixed with 70% ethanol in PBS at -20°C overnight, washed with PBS and incubated at a density of $1\text{--}2 \times 10^6$ cells/ml with 50 $\mu\text{g}/\text{ml}$ propidium iodide (PI) in PBS at room temperature in the dark for 10 min. DAPI fluorescence of cells was assayed by flow cytometry in the BD Accuri™ C6 Flow Cytometer (BD Biosciences, Franklin Lakes, USA).

Cell proliferation assay

The A549 cells were seeded at 1000 cells per well into a 96-well plate (Corning Co, Corning, USA) and cultured at 37°C in 5% CO_2 . Twenty-four hours after transfection with 20 nM miR-30a mimics or mimics NC, cell proliferation was assessed every 24 h by the 3-(4,5-dimethylthiazol-2-yl)-5-(3-carboxymethoxyphenyl)-2-(4-sulphophenyl)-

2H-tetrazolium (MTS) assay using CellTiter 96 Aqueous One Solution Cell Proliferation Assay Kit (Promega, Madison, USA) according to the manufacturer's instructions. Briefly, MTS reagent solution was added to each well and incubated at 37°C in 5% CO_2 for 2 h. Cell proliferation was assessed by measuring the absorbance at 490 nm with a SpectraMax 340PC384 Microplate Reader (Molecular Devices, Sunnyvale, USA). Triplicate wells were measured for cell viability in each treatment group.

Wound-healing assay

The wound-healing assay mimics tumor cell migration *in vivo*. The A549 cells were seeded in a 6-well plate at a density of $0.5\text{--}1 \times 10^6$ cells/well, and after 24 h of growth they should reach $\sim 90\%$ confluence as a monolayer. Then, cells were transfected with 20 nM miR-30a mimics or *EYA2* siRNAs and their corresponding negative control. Then, the cells were cultured in DMEM with 2% FBS (low-serum culture media) for 12 h. The monolayer was scratched gently and slowly with a yellow pipette tip across the center of the well. After scratching, the detached cells were washed away with phosphate-buffered saline (PBS). The remaining cells were cultured for additional 48 h in fresh low-serum culture media to allow wound healing. At 0 and 48 h, images were captured on a photomicroscope (Olympus, Tokyo, Japan) at a magnification of $\times 200$. The migration ability of the cells was assessed by counting the wound closure rate.

Matrigel invasion assay

The A549 cells were harvested 24 h after transfection with 20 nM miR-30a mimics or *EYA2* siRNAs and their corresponding negative

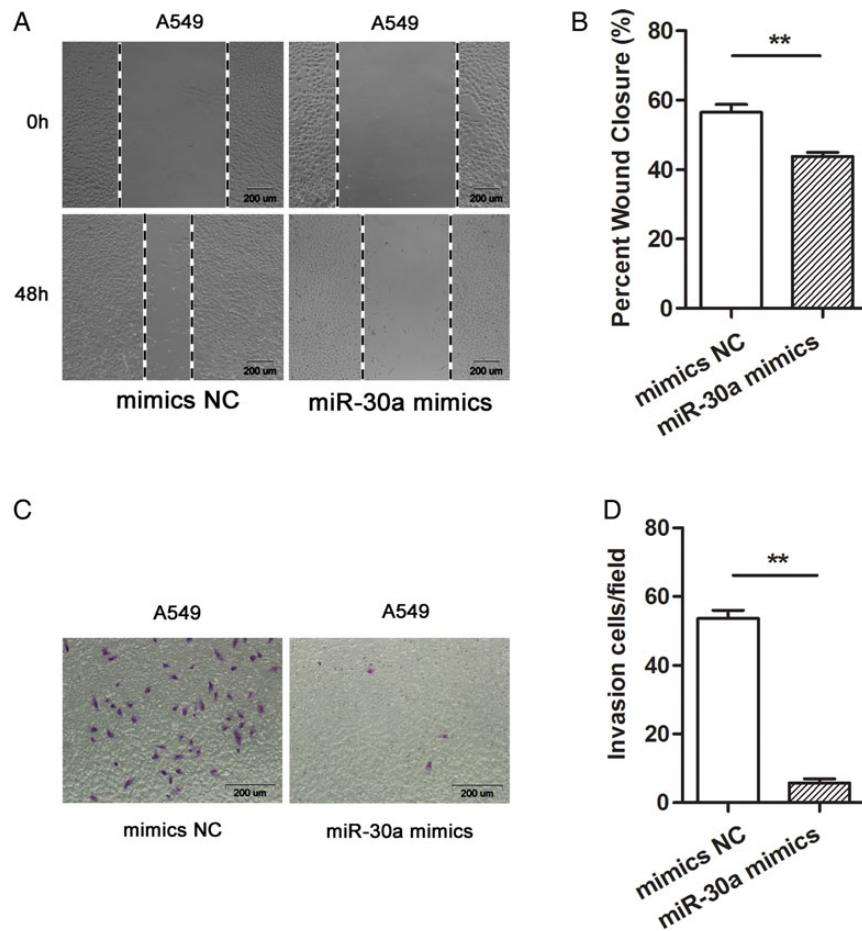


Figure 3. Overexpression of miR-30a in A549 cells inhibited migration and invasion of the cells (A) The wound-healing assay of A549 cells transfected with 20 nM mimics NC or miR-30a mimics, respectively. (B) The rate of wound closure \pm SE was shown. The experiment was performed in triplicate with similar trend. (C) A549 cells transfected with 20 nM mimics NC or miR-30a mimics, respectively, were seeded into the up chambers at 8000 cells per well. After culturing for 24 h, the invasive cells were stained by Giemsa. Representative fields of invasive cells on membrane are captured. (D) The average number of invasive cells per field from three independent experiments \pm SE was shown. $**P < 0.01$.

control, resuspended in FBS-free DMEM culture medium. Transwell chambers with 0.8- μ m pore size filter (Corning) were coated with 30 μ g of matrigel (BD Biosciences) and dried for 60 min at 37°C. The lower chamber was filled with 750 μ l DMEM culture medium containing 10% FBS, and the upper chamber was seeded with 8000 cells from each treatment. Then, the chambers in 24-well plate were incubated at 37°C in 5% CO₂ for 24 h. After incubation, cells that had entered the lower surface of the filter membrane were fixed with 3.7% formaldehyde solution for 2 min, permeabilized by 100% methanol for 20 min, stained by Giemsa for 15 min at room temperature and washed with PBS. Cells remaining on the upper chamber (non-invaded) were scraped off gently with a cotton swab. The images of six random fields on the lower surfaces (with invasive cells) were captured by the photomicroscope at a magnification of $\times 200$. The cells in each field were counted.

Dual-luciferase reporter assay

To simplify our cloning strategy, the oligonucleotides in the 3' UTR of the *EYA2* mRNA (position 2592-2702, NM_005244.4) which contains the seed sequence of the miR-30a were synthesized using a chemical-based oligonucleotide synthesis method (Sangon Biotech, Shanghai, China). As a negative control, oligonucleotides containing a mutated miR-30a targeting site were also designed. The mutants

were created by replacing the seed regions of the miR-30a targeting site with complementary bases. The restriction enzyme cleavage sites of *Xho*I and *Xba*I in the multiple cloning site (MCS) of the pGLO dual-luciferase miRNA target expression vector (Promega) were chosen as cloning sites. The oligonucleotides were inserted downstream of the firefly luciferase gene in pGLO vector, and the resulting plasmids were designated as pGLO-*EYA2*-wild-type and pGLO-*EYA2*-mutant, respectively. Renilla luciferase gene fused into pGLO vector was used as an internal control. The ligated product was transduced into DH5 α (TaKaRa). After 12 h of amplification at 37°C in a shaker (Thermo Fisher Scientific), the total plasmids were extracted from DH5 α solution by the plasmid purification kit (QIAGEN) and sequenced (Sain Biological Corporation, Shanghai, China). For the luciferase reporter assay, A549 cells were co-transfected in a 24-well plate with 200 ng of the recombinant plasmids and 20 nM miR-30a mimics per well. Twenty-four hours after co-transfection, cell lysates were collected and luciferase activities were measured using a Dual-Luciferase Reporter System (Promega).

Western blot analysis

Cells were lysed on ice with lysis buffer containing protease inhibitors, phosphatase inhibitors, and phenylmethylsulfonyl fluoride. The lysates were clarified by centrifugation at 20,400 g for 10 min at

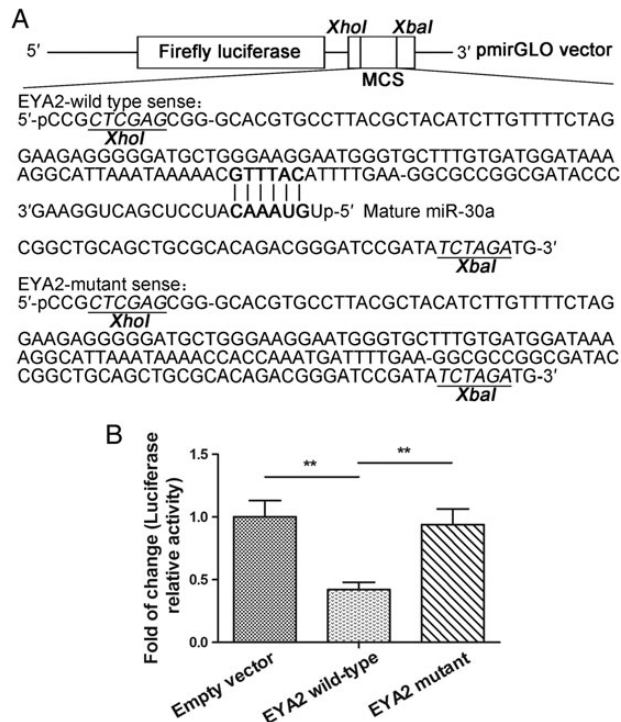


Figure 4. EYA2 gene is a direct downstream target of miR-30a in A549 cells
 (A) The EYA2-wild-type with putative binding site of miR-30a and the mutant generated by replacing the seed region of miR-30a with complementary bases were cloned into the pmirGLO vector, respectively. The restriction enzyme cutting sites of the *XhoI* and *XbaI* were chosen as the cloning sites. (B) For luciferase assay, A549 cells were transiently cotransfected with 200 ng luciferase vectors and 50 nM miR-30a mimics. Luciferase activities were measured 24 h after transfection. Firefly luciferase activities were normalized by the activity of renilla luciferase. The experiments were performed in triplicate with similar trend. ** $P < 0.01$.

4°C, and the supernatants were collected. For each sample, 15 µg of total protein was electrophoresed on a 12% sodium dodecyl sulfate polyacrylamide gel electrophoresis followed by an electrophoretic transfer to a polyvinyl difluoride membrane (Millipore, Massachusetts, USA). After being blocked for 60 min with Tris-buffered saline (TBS) containing 0.1% Tween-20 (TBST) and 5% bovine serum albumin (BSA) at room temperature, the membranes were incubated with primary antibodies at 4°C overnight in 5% BSA, washed thrice with TBST, and then incubated with the corresponding horseradish peroxidase conjugate secondary antibody. The following primary antibodies were used: rabbit monoclonal anti-EYA2 antibody (Abcam, Cambridge, USA) at a dilution of 1:10,000; mouse monoclonal anti-GAPDH antibody (Abcam) at a dilution of 1:2000; rabbit monoclonal anti-p27 KIP1 antibody (Abcam) at a dilution of 1:2000; rabbit monoclonal anti-Cyclin E1 antibody (Abcam) at a dilution of 1:2000; rabbit polyclonal anti-Cyclin A1 antibody (BOSTER, Wuhan, China) at a dilution of 1:2000; and rabbit polyclonal anti-Cyclin D1 antibody (BOSTER) at a dilution of 1:2000. All bands were detected using an enhanced chemiluminescence (ECL) kit (Thermo Fisher Scientific).

Immunohistochemistry

Lung adenocarcinoma FFPE tissues were cut into 4-µm thick sections. The sections were pretreated at room temperature for 1 h, then dewaxed in xylene, rehydrated in graded ethanol, and washed with PBS solution. Antigen retrieval was performed at 100°C for 20 min

in a 10 mM citrate buffer (pH 6.0), and endogenous peroxidase activity was quenched by using 3% hydrogen peroxide in methanol for 10 min at room temperature. After being washed with PBS solution, sections were blocked with 10% normal goat serum for 10 min at room temperature. Then, the sections were incubated with a rabbit polyclonal anti-EYA2 antibody (Abcam) at a dilution of 1:1500 at 4°C overnight, followed by incubation with an anti-rabbit secondary antibody for 30 min at room temperature. Slides were then processed using 3,3-diaminobenzidine (DAB) and counterstained with hematoxylin. Finally, the degree of immunoreactivity for *EYA2* expression was evaluated semiquantitatively on the basis of staining intensity and the proportion of positive tumor cells. The staining intensity was graded as follows: 0 (no staining), 1 (light yellow), 2 (yellowish brown), and 3 (brown). The positive cells were graded according to the percentage of positive cells as follows: 0 (no positive tumor cells), 1 (<10% positive tumor cells), 2 (11%–50% positive tumor cells), 3 (51%–80% positive tumor cells), and 4 (>80% positive tumor cells). The percentage of positive cells and the staining intensity were then multiplied to generate the immunoreactivity score.

Overexpression vector construction and rescue experiment

The empty vector and pDoubleEx-EGFP-EYA2 expression vector were obtained from YRGene Bioresource Center (Changsha, China). To examine the transfection efficiency, enhanced green fluorescent protein (EGFP) expression in A549 cells was observed by an inverted fluorescence microscope (Olympus) at 48 h after transfection. Meanwhile, the cells were stained with Hoechst 33258 (Thermo Fisher Scientific). For a functional rescue experiment, A549 cells were cotransfected with p-EYA2 (2 µg) + miR-30a mimics (40 nM), p-EYA2 (2 µg) + mimics NC (40 nM), p-empty (2 µg) + miR-30a mimics (40 nM), and p-empty (2 µg) + mimics NC (40 nM), respectively, in a 6-well plate, and then the cells were used for the wound-healing assay and matrigel invasion assay as described previously.

Statistical analysis

The $2^{-\Delta\Delta Ct}$ method was used to analyze the relative changes in miR-30a expression from qRT-PCR experiments as described previously [25]. For the wound-healing assay, Image-Pro Plus 6.0 software (MediaCybernetics, Rockville, USA) was used to analyze the percentage of wound closure. ModFit LT 4.1 software (Verity, Topsham, USA) was used to analyze the cell cycle distribution of cells. All charts were generated by GraphPad Prism 5 software (GraphPad, La Jolla, USA). Differences in the numerical data between the cancer and adjacent normal tissues were analyzed by paired Student's *t*-test. Other data were evaluated with one-way analysis of variance (ANOVA). All data were presented as the mean ± standard error (SE). A *P* value <0.05 was considered to be statistically significant.

Results

miR-30a was downregulated in lung adenocarcinoma cells and tissues

To confirm the relevance of miR-30a expression in NSCLC, the level of miR-30a was determined in A549 and BEAS-2B cell lines and quantified in 14 matched normal lung and lung cancer tissues by qRT-PCR. The result from qRT-PCR showed that the relative expression level of miR-30a in A549 cells is significantly reduced compared with that in the BEAS-2B cells (Fig. 1A, $P < 0.01$). Correspondingly, miR-30a is also significantly decreased in lung adenocarcinoma tissues compared that in the matched normal tissues (Fig. 1B, $P < 0.01$). As our sample

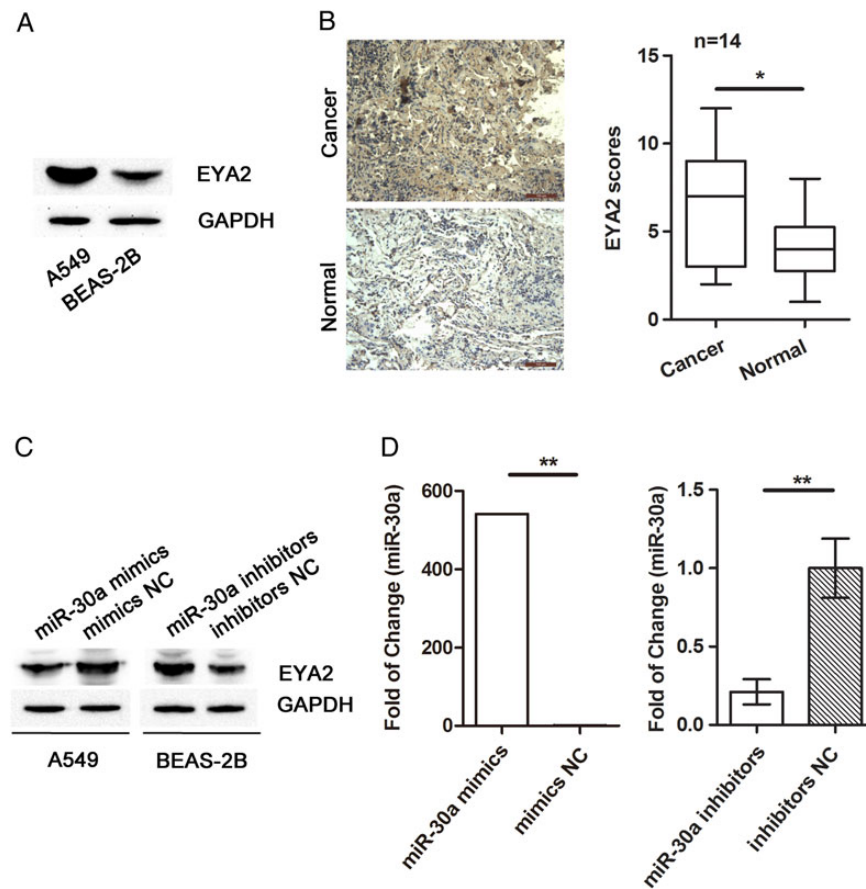


Figure 5. miR-30a suppresses EYA2 protein expression (A) The results of the western blot of the proteins extracted from the A549 and BEAS-2B cell lines. GAPDH was used as an internal reference protein for loading control. (B) Immunohistochemical analysis of EYA2 expression in 14 pairs of lung adenocarcinoma or the corresponding normal lung tissues ($\times 200$). (C) The A549 and BEAS-2B cells were transfected with 50 nM mimics NC, inhibitors NC, miR-30a mimics or inhibitors and cultured for additional 48 h. The cells were digested by trypsin for western blot analysis. The protein levels were normalized by GAPDH. (D) The fold of change of miR-30a expression in A549 or BEAS-2B cells under the same conditions was evaluated by qRT-PCR. The experiments were repeated at least three times with similar trends. * $P < 0.05$, ** $P < 0.01$.

size is modest, we also obtained a suitable dataset GSE63805 (Robles AI and Harris, 2015), which include 30 pairs of lung adenocarcinoma and adjacent normal tissue samples from the Gene Expression Omnibus (GEO) to compare the level of miR-30a between lung adenocarcinoma and its normal counterpart. The analysis result from dataset GSE63805 supported our results (Fig. 1C, $P < 0.01$).

Overexpression of miR-30a in A549 cell line had no effect on cell proliferation and cell cycle progression

To investigate whether miR-30a regulates A549 cell proliferation, cells were transfected with miR-30a mimics or mimics NC, and cell proliferation was analyzed by the MTS assay every 24 h after transfection for 5 days (Fig. 2A). The result indicated that miR-30a overexpression did not inhibit the cell proliferation of A549 cells compared with the mimics NC. To investigate whether miR-30a modulates cell cycle progression in A549 cells, flow cytometry was used to measure cell cycle distribution in cells overexpressing miR-30a mimics or mimics NC. Forty-eight hours after transfection, A549 cells were used for cell cycle analysis. The cell cycle analysis results showed that miR-30a mimics (66.20%) did not significantly induce G1 to S arrest compared with the mimics NC (66.13%) (Fig. 2B). In addition, the effects of miR-30a on the expression of four cell cycle-related genes (*p27 kip1*, *cyclin D1*, *cyclin E1*, and *cyclin A1*) were also examined.

The results showed that miR-30a overexpression did not alter the expressions of the above-mentioned genes compared with the mimics NC (Fig. 2C). Taken together, all these results indicated that overexpression of miR-30a in A549 cells had no significant effect on cell proliferation and cell cycle progression.

Overexpression of miR-30a in A549 cell line inhibited migration and invasion

To determine whether miR-30a inhibited migration of lung adenocarcinoma cells, wound-healing assay was performed. The result revealed that the increase of miR-30a expression inhibited A549 cell mobility (Fig. 3A) compared with the mimics NC. The migration capability of A549 cells was also assessed by measuring the rate of wound closure (Fig. 3B). To further explore whether miR-30a regulated A549 cell invasion, a transwell assay was performed. A549 cells transfected with mimics NC or miR-30a mimics were seeded into the up chambers with 8- μm pore size polycarbonate membranes, and their invasive potential was estimated after 24 h of culture. The images on the lower surfaces of the chambers (with invaded cells) were captured (Fig. 3C) and quantified (Fig. 3D). The results showed that the invasion capacity of A549 cells overexpressing miR-30a was significantly reduced compared with the mimics NC. All these data suggested that overexpression of miR-30a in A549 cells inhibited migration and invasion.

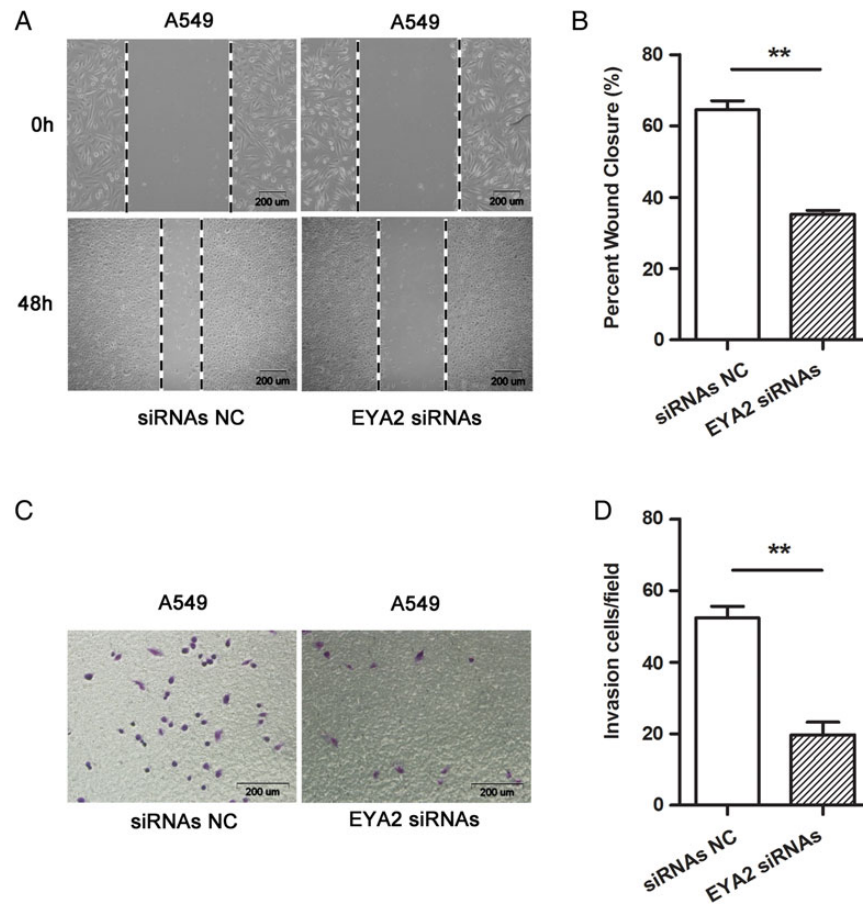


Figure 6. Downregulation of *EYA2* in A549 cells suppressed migration and invasion of the cells (A) The wound-healing assay of A549 cells transfected with 20 nM siRNAs NC or *EYA2* siRNAs, respectively. (B) The rate of wound closure \pm SE was shown. The experiment was performed in triplicate with similar trend. (C) The transwell cell invasion assay of A549 cells transfected with 20 nM siRNAs NC or *EYA2* siRNAs, respectively. Representative fields of invasive cells on membrane are captured. (D) The average number of invasive cells per field from three independent experiments \pm SE was shown. ** $P < 0.01$.

miR-30a inhibited *EYA2* expression by targeting its 3' UTR in A549 cells

To confirm if *EYA2* gene was a direct target of miR-30a, a dual-luciferase reporter assay was performed in the A549 cells. The partial sequence of the 3' UTR of the *EYA2* mRNA was synthesized with the putative miR-30a binding site. A fragment with the same part of *EYA2* mRNA 3' UTR but with miR-30a binding site replaced by complementary bases was also designed. The two fragments were cloned into a dual-luciferase report vector, respectively, and the resulting plasmids were designated as pGLO-*EYA2*-wild-type and pGLO-*EYA2*-mutant (Fig. 4A). Recombinant plasmids (200 ng) were transfected into A549 cells along with 50 nM miR-30a mimics for 24 h. The results showed that miR-30a strongly inhibited the activity of the firefly luciferase gene of the reporter vector containing the *EYA2* 3' UTR with a wild-type miR-30a binding site, but did not inhibit the reporter vector with mutant *EYA2* 3' UTR (Fig. 4B). This result indicated that miR-30a inhibited the expression of *EYA2* by directly targeting its 3' UTR.

miR-30a inhibited the expression of *EYA2* protein in A549 cells

To examine the expression of *EYA2* gene in lung adenocarcinoma, the protein level of *EYA2* was assessed by western blotting and immunohistochemistry. It was found that *EYA2* was significantly

upregulated both in A549 cells (Fig. 5A) and in lung adenocarcinoma tissues from 14 patients (Fig. 5B). To elucidate the regulatory relationship between miR-30a and *EYA2* expression in lung adenocarcinoma, miR-30a mimics and its inhibitors were transfected into A549 and BEAS-2B cell lines, respectively. The cell lysates were analyzed by western blot analysis. The results showed that the expression level of *EYA2* protein was significantly decreased in A549 cell line and increased in the BEAS-2B cell line after transfection with miR-30a mimics and its inhibitors (Fig. 5C), respectively. Meanwhile, the miR-30a expression was evaluated by qRT-PCR to assess the transfection rate. The bar charts showed that levels of miR-30a were increased by its mimics and decreased by its inhibitors (Fig. 5D) as expected. All these data demonstrated that *EYA2* was a direct target of miR-30a in lung adenocarcinoma cells.

miR-30a inhibited migration and invasion of A549 cells via targeting *EYA2*

To explore whether the functional effect of miR-30a on A549 cell line was dependent on *EYA2* gene, an RNA interference experiment and a rescue experiment were performed. The results from RNA interference experiment revealed that the decrease of *EYA2* expression by transfection with *EYA2* specific siRNAs in A549 cells inhibited migration (Fig. 6A,B) and invasion (Fig. 6C,D) compared with their corresponding negative control. Subsequently, a rescue experiment by

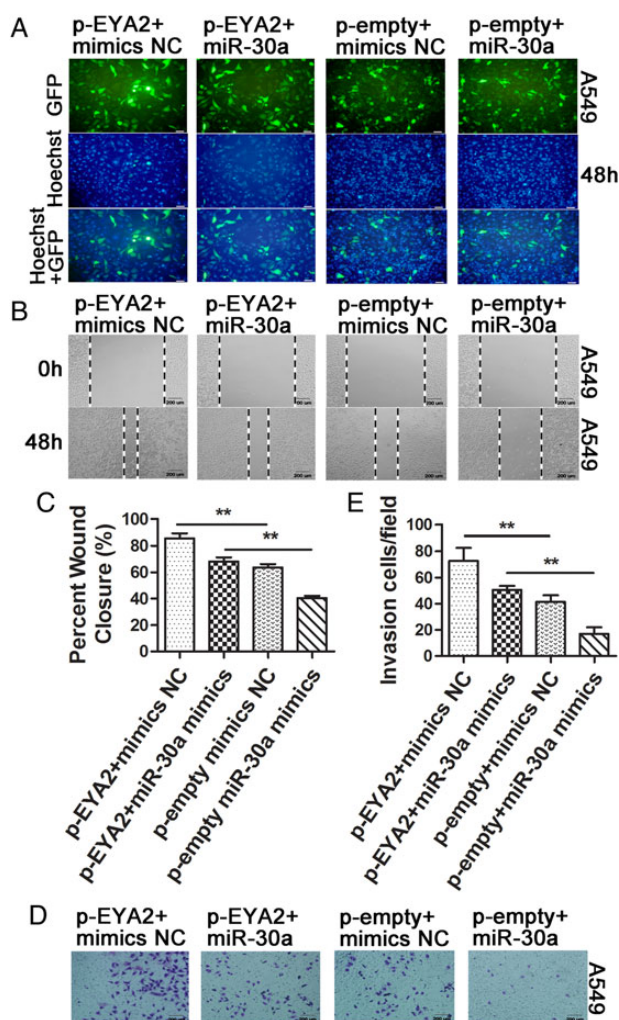


Figure 7. Overexpression of *EYA2* reverses the inhibition of cell invasion and migration induced by upregulated miR-30a in A549 cells (A) The expression of EGFP cotransfected with p-*EYA2* + mimics NC, p-*EYA2* + miR-30a mimics, p-empty + mimics NC, or p-empty + miR-30a mimics for 48 h was observed using a fluorescent inverted microscope ($\times 200$). Hoechst was used for cell staining. (B,C) Wound-healing assay and (D,E) matrigel invasion assay demonstrated functional effects in A549 cells after cotransfection. Experimental values presented as the mean \pm SE. The experiments were repeated at least three times with similar trends. $**P < 0.01$.

upregulating the expression of *EYA2* with an *EYA2* expression vector in A549 cells was performed. The fluorescence microscopy was used to evaluate the transfection efficiency of p-*EYA2* + miR-30a mimics, p-*EYA2* + mimics NC, p-empty + miR-30a mimics, and p-empty + mimics NC (Fig. 7A). The results from the rescue experiments showed that upregulation of *EYA2* protein promoted migration (Fig. 7B,C) and invasion (Fig. 7D,E) of A549 cells, and to a certain extent reversed the inhibition of cell migration (Fig. 7B,C) and invasion (Fig. 7D,E) induced by miR-30a mimics. These results suggested that miR-30a targeted *EYA2* directly, resulting in inhibition of migration and invasion in lung adenocarcinoma A549 cell line.

Discussion

This study sought to determine the biological function of miR-30a on the pathogenesis of the NSCLC and the potential mechanism by which

miR-30a inhibited *EYA2* expression. We found that: (i) miR-30a was downregulated but *EYA2* was upregulated in the lung adenocarcinoma cell line A549 and lung adenocarcinoma tissues; (ii) overexpression of miR-30a in the lung adenocarcinoma cells of A549 inhibited the migration and invasion but not cell proliferation and cell cycle progression; (iii) miR-30a suppressed the expression of *EYA2* by targeting its mRNA 3' UTR in A549 cells; (iv) the expression of *EYA2* protein was inversely correlated with miR-30a expression in the lung adenocarcinoma cell line of A549 and normal lung/bronchus epithelia cell line of BEAS-2B; (v) downregulation of *EYA2* protein inhibited the invasion and migration of A549 cells; and (vi) upregulation of *EYA2* protein partially reverses the inhibition of cell invasion and migration induced by upregulated miR-30a in A549 cells.

Evidence has shown that miR-30a was closely related to multiple malignant phenotypes of human cancers. Baraniskin *et al.* [4] found that miR-30a suppressed the cell growth and modulated the cell cycle in colon cells. Zhong *et al.* [3] found that overexpression of miR-30a suppressed CRC colorectal carcinoma cell migration and invasion *in vitro*. Jia *et al.* [12] found that overexpression of miR-30a in LN229 or SNB19 glioblastoma cells promoted cell growth and invasion. In addition, Huang *et al.* [15] showed that overexpression of miR-30a in the A549 cells did not alter the cell cycle, proliferation but promoted migration. However, cell proliferation, cell cycle progression and migration are just three of the main characteristics of the malignant phenotypes of human cancer cells. Invasion is another main characteristic of the malignant phenotypes, and the effect of overexpression of miR-30a on invasion in lung adenocarcinoma has not been reported. Our results indicated that overexpression of miR-30a in lung adenocarcinoma A549 cell line inhibited the migration and invasion but not cell proliferation and cell cycle progression, which is contradictory to the previous conclusion by Patnaik *et al.* [15] that miR-30a did not affect the malignant phenotype of lung adenocarcinoma A549 cell line. This phenomenon is partially due to the variety of the multiphenotypes of malignant cells. Although miR-30a has no effect on cell proliferation and cell cycle progression, it did show an inhibitory effect on the migration and invasion. Thus, to study the effect of miR-30a on malignant phenotype of cancer cells, various phenotypes should be examined together so that more objective and comprehensive conclusions can be drawn from these results. The evaluation on cell phenotypes, such as cell proliferation, cell cycle progression, migration, and invasion, may be useful to guide the future study about the effect of miRNAs on cancer cells.

Previously, a number of predicted targets of miR-30a have been reported in various cancers. These genes include *PIK3CD* [3], *VIM* [10], *SEPT7* [12], *DLL4* [9], *CD99* [8], *LOX* [7], *DTL* [4], *IRS2* [5], *FOX L2* [13], etc. In addition, the signaling pathways of miR-30a implicated in the pathogenesis of cancers have also been reported. Zhao *et al.* [26] found that miR-30a functions as a tumor suppressor by targeting the oncogenic Wnt/beta-catenin/BCL9 pathway in H929 cells. Che *et al.* [27] found that miR-30 overexpression promoted glioma stem cells by regulating the Jak/STAT3 signaling pathway. miR-30a activity was also found to be regulated by competitive endogenous RNA (ceRNA). Liu *et al.* [28] found that *AEG-1* 3' UTR functions as a ceRNA, inducing epithelial-mesenchymal transition of human NSCLC, by regulating miR-30a activity. However, the mechanism by which miR-30a plays a role in lung adenocarcinoma is still unknown. Fu *et al.* [6] demonstrated that miR-30a inhibited breast cancer cell proliferation and migration by downregulating *EYA2*. To examine if this mechanism can be also applied to lung adenocarcinoma, we investigated if *EYA2* 3' UTR was the direct target of miR-30a and if *EYA2* expression was downregulated by miR-30a.

We found that the activities of firefly luciferase cloned with the EYA2 3' UTR were inhibited by miR-30a and overexpression of miR-30a suppressed the expression of EYA2 in lung adenocarcinoma A549 cell line. These results suggested that EYA2 is a direct target of miR-30a in lung adenocarcinoma A549 cells. Pandey *et al.* [17] found that EYA2 protein can promote proliferation, transformation, migration, and invasion of breast cancer cells. Our study revealed that the downregulation of EYA2 protein level inhibited the migration and invasion of A549 cells and the upregulation of EYA2 protein level partially reversed the inhibition of cell invasion and migration induced by upregulated miR-30a in A549 cells. Therefore, it is possible that miR-30a inhibited migration and invasion of lung adenocarcinoma A549 cell line by suppressing the expression of EYA2. In summary, our findings have provided a potential mechanism by which miR-30a suppressed migration and invasion of the lung adenocarcinoma cells.

Funding

This work was supported by the grants from the National Natural Science Foundation of China (Nos. 81372360 and 81460435) and the Key Projects of Applied Basic Research of Yunnan Province (No. 2014FA022).

References

- He J, Chen WQ. *Chinese Cancer Registry Annual Report 2012*. 1st edn. Beijing: Military Medical Press, 2012, 72–75.
- Zhang B, Wang Q, Pan X. MicroRNAs and their regulatory roles in animals and plants. *J Cell Physiol* 2007, 210: 279–289.
- Zhong M, Bian Z, Wu Z. miR-30a suppresses cell migration and invasion through downregulation of PIK3CD in colorectal carcinoma. *Cell Physiol Biochem* 2013, 31: 209–218.
- Baraniskin A, Birkenkamp-Demtroder K, Maghnoouj A, Zollner H, Munding J, Klein-Scory S, Reinacher-Schick A, *et al.* miR-30a-5p suppresses tumor growth in colon carcinoma by targeting DTL. *Carcinogenesis* 2012, 33: 732–739.
- Zhang Q, Tang Q, Qin D, Yu L, Huang R, Lv G, Zou Z, *et al.* Role of microRNA 30a targeting insulin receptor substrate 2 in colorectal tumorigenesis. *Mol Cell Biol* 2015, 35: 988–1000.
- Fu J, Xu X, Kang L, Zhou L, Wang S, Lu J, Cheng L, *et al.* miR-30a suppresses breast cancer cell proliferation and migration by targeting Eya2. *Biochem Biophys Res Commun* 2014, 445: 314–319.
- Boufraquech M, Nilubol N, Zhang L, Gara SK, Sadowski SM, Mehta A, He M, *et al.* miR30a inhibits LOX expression and anaplastic thyroid cancer progression. *Cancer Res* 2015, 75: 367–377.
- Franzetti GA, Laud-Duval K, Bellanger D, Stern MH, Sastre-Garau X, Delattre O. miR-30a-5p connects EWS-FLI1 and CD99, two major therapeutic targets in Ewing tumor. *Oncogene* 2013, 32: 3915–3921.
- Huang QB, Ma X, Zhang X, Liu SW, Ai Q, Shi TP, Zhang Y, *et al.* Down-regulated miR-30a in clear cell renal cell carcinoma correlated with tumor hematogenous metastasis by targeting angiogenesis-specific DLL4. *PLoS one* 2013, 8: e67294.
- Liu Z, Chen L, Zhang X, Xu X, Xing H, Zhang Y, Li W, *et al.* RUNX3 regulates vimentin expression via miR-30a during epithelial–mesenchymal transition in gastric cancer cells. *J Cell Mol Med* 2014, 18: 610–623.
- Wang H-Y, Li Y-Y, Fu S, Wang X-P, Huang M-Y, Zhang X, Shao Q, *et al.* MicroRNA-30a promotes invasiveness and metastasis *in vitro* and *in vivo* through epithelial–mesenchymal transition and results in poor survival of nasopharyngeal carcinoma patients. *Exp Biol Med* 2014, 239: 891–898.
- Jia Z, Wang K, Wang G, Zhang A, Pu P. miR-30a-5p antisense oligonucleotide suppresses glioma cell growth by targeting SEPT7. *PLoS one* 2013, 8: e55008.
- Wang T, Li F, Tang S. miR-30a upregulates BCL2A1, IER3 and cyclin D2 expression by targeting FOXL2. *Oncol Lett* 2015, 9: 967–971.
- Yanaihara N, Caplen N, Bowman E, Seike M, Kumamoto K, Yi M, Stephens RM, *et al.* Unique microRNA molecular profiles in lung cancer diagnosis and prognosis. *Cancer Cell* 2006, 9: 189–198.
- Patnaik SK, Kannisto E, Yendamuri S. Overexpression of microRNA miR-30a or miR-191 in A549 lung cancer or BEAS-2B normal lung cell lines does not alter phenotype. *PLoS one* 2010, 5: e9219.
- Laclef C. The transcriptional activator Eya is a tyrosine phosphatase. *Med Sci (Paris)* 2004, 20: 617–619.
- Pandey RN, Rani R, Yeo EJ, Spencer M, Hu S, Lang RA, Hegde RS. The eyes absent phosphatase-transactivator proteins promote proliferation, transformation, migration, and invasion of tumor cells. *Oncogene* 2010, 29: 3715–3722.
- Krueger AB, Drasin DJ, Lea WA, Patrick AN, Patnaik S, Backos DS, Matheson CJ, *et al.* Allosteric inhibitors of the Eya2 phosphatase are selective and inhibit Eya2-mediated cell migration. *J Biol Chem* 2014, 289: 16349–16361.
- Bierkens M, Krijgsman O, Wilting SM, Bosch L, Jaspers A, Meijer GA, Meijer CJ, *et al.* Focal aberrations indicate EYA2 and hsa-miR-375 as oncogene and tumor suppressor in cervical carcinogenesis. *Genes Chromosomes Cancer* 2013, 52: 56–68.
- Vincent A, Hong SM, Hu C, Omura N, Young A, Kim H, Yu J, *et al.* Epigenetic silencing of EYA2 in pancreatic adenocarcinomas promotes tumor growth. *Oncotarget* 2014, 5: 2575–2587.
- Zou H, Harrington JJ, Shire AM, Rego RL, Wang L, Campbell ME, Oberg AL, *et al.* Highly methylated genes in colorectal neoplasia: implications for screening. *Cancer Epidemiol Biomarkers Prev* 2007, 16: 2686–2696.
- Zhang L, Yang N, Huang J, Buckanovich RJ, Liang S, Barchetti A, Vezzani C, *et al.* Transcriptional coactivator Drosophila eyes absent homologue 2 is up-regulated in epithelial ovarian cancer and promotes tumor growth. *Cancer Res* 2005, 65: 925–932.
- Guo JT, Ding LH, Liang CY, Zhou NK, Ye QN. Expression of EYA2 in non-small cell lung cancer. *Zhonghua Zhong Liu Za Zhi* 2009, 31: 528–531.
- Chen C, Ridzon DA, Broomer AJ, Zhou Z, Lee DH, Nguyen JT, Barbisin M, *et al.* Real-time quantification of microRNAs by stem-loop RT-PCR. *Nucleic Acids Res* 2005, 33: e179.
- Livak KJ, Schmittgen TD. Analysis of relative gene expression data using real-time quantitative PCR and the 2^{(-Delta Delta C(T))} method. *Methods* 2001, 25: 402–408.
- Zhao JJ, Lin J, Zhu D, Wang X, Brooks D, Chen M, Chu ZB, *et al.* miR-30-5p functions as a tumor suppressor and novel therapeutic tool by targeting the oncogenic Wnt/beta-catenin/BCL9 pathway. *Cancer Res* 2014, 74: 1801–1813.
- Che S, Sun T, Wang J, Jiao Y, Wang C, Meng Q, Qi W, *et al.* miR-30 overexpression promotes glioma stem cells by regulating Jak/STAT3 signaling pathway. *Tumour Biol* 2015, 36: 6805–6811.
- Liu K, Guo L, Guo Y, Zhou B, Li T, Yang H, Yin R, *et al.* AEG-1 3'-untranslated region functions as a ceRNA in inducing epithelial–mesenchymal transition of human non-small cell lung cancer by regulating miR-30a activity. *Eur J Cell Biol* 2015, 94: 22–31.